









Global constraint on the magnitude of anomalous chiral effects in heavy-ion collisions

Wen-Ya Wu ^{1,2} Qi-Ye Shou ^{1,2,*} Panos Christakoglou,^{3,†} Prottay Das,⁴ Md. Rihan Haque ⁵ Guo-Liang Ma ^{1,2}
Yu-Gang Ma ^{1,2,‡} Bedangadas Mohanty,⁴ Chun-Zheng Wang ^{1,2} Song Zhang ^{1,2} and Jie Zhao ^{1,2}

¹Key Laboratory of Nuclear Physics and Ion-Beam Application (MOE), Institute of Modern Physics, Fudan University, Shanghai 200433, China

²Shanghai Research Center for Theoretical Nuclear Physics, NSFC and Fudan University, Shanghai 200438, China

³Nikhef, Nationaal Instituut voor Subatomaire Fysica, 1098 XG Amsterdam, The Netherlands

⁴National Institute of Science Education and Research, Homi Bhabha National Institute, Jatni, Khurda 752050, India

⁵Warsaw University of Technology, 00-661 Warsaw, Poland



(Received 28 November 2022; accepted 2 March 2023; published 21 March 2023)

When searching for anomalous chiral effects in heavy-ion collisions, one of the most crucial points is the relationship between the signal and the background. In this Letter, we present a simulation in a modified blast wave model at CERN Large Hadron Collider energy, which can simultaneously characterize the majority of measurable quantities, in particular, the chiral magnetic effect (CME) and the chiral magnetic wave (CMW) observables. Such a universal description, naturally and quantitatively unifies the CME and the CMW studies and brings to light the connection with the local charge conservation (LCC) background. Moreover, a simple phenomenological approach is performed to introduce the signals, aiming at quantifying the maximum allowable strength of the signals within experimental precision. Such a constraint provides a novel perspective to understand the experimental data and sheds new light on the study of anomalous chiral effects as well as charge dependent correlations.

DOI: [10.1103/PhysRevC.107.L031902](https://doi.org/10.1103/PhysRevC.107.L031902)

Introduction. Collisions between heavy ions at ultrarelativistic energies have been extensively used in the last decades to study the transition to a deconfined state of matter, the quark gluon plasma (QGP). This transition, according to quantum chromodynamics (QCD) calculations on the lattice, is expected to take place at energy densities and temperatures which are accessible in the laboratories such as the BNL Relativistic Heavy Ion Collider (RHIC) and the CERN Large Hadron Collider (LHC). In addition, such collisions provide the unique opportunity to test novel QCD phenomena that are directly connected to the rich structure of the vacuum of the theory [1,2]. These phenomena are associated with transitions that lead to chirality imbalance and consequently to \mathcal{P} (parity) and/or \mathcal{CP} (charge-parity) violating effects in strong interactions [3–9]. Theoretical studies highlighted that in the presence of an external strong magnetic field, like the one generated at the initial stages of a heavy ion collision [10–12], such transitions can lead to the development of macroscopic phenomena such as the chiral magnetic effect (CME) [9,13–15] and the chiral magnetic wave (CMW) [16–19]. Both the CME and the CMW are argued to have an experimentally accessible signal, see Refs. [20–24] for the latest review.

Specifically, the CME is theorized to manifest itself in a finite electric dipole moment in the QGP and develops along

the direction of the magnetic field. Taking advantage of the azimuthal emission of final state hadrons, it is feasible to detect the CME-induced signal via the correlators of $\gamma \equiv \cos(\phi_\alpha + \phi_\beta - 2\Psi)$ and $\delta \equiv \cos(\phi_\alpha - \phi_\beta)$ [13,25], where ϕ_α and ϕ_β are azimuthal angles of two particles of interest, and Ψ is that of the reaction plane, the plane defined by the impact parameter between the two colliding nuclei and the beam axis. This measurement is usually performed with the same-sign (SS) and opposite-sign (OS) charge combinations of α and β , and their differences are used to explore the possible signal

$$\Delta\gamma \equiv \gamma_{\text{OS}} - \gamma_{\text{SS}}, \quad \Delta\delta \equiv \delta_{\text{OS}} - \delta_{\text{SS}}. \quad (1)$$

Meanwhile, the CMW is expected to create an electric quadrupole moment in the participant region, where the “poles” (out of plane) and the “equator” (in plane), respectively, acquire additional positive or negative charges [16]. Such an effect can be probed by the charge asymmetry (A_{ch}) dependence of elliptic flow (v_2) between the positively and negatively charged particles:

$$\Delta v_2 \equiv v_2^- - v_2^+ \simeq r A_{\text{ch}}, \quad (2)$$

where $A_{\text{ch}} \equiv (N^+ - N^-)/(N^+ + N^-)$ with N denoting the number of particles in a given event, and the slope r is used to quantify the signal.

Over the past decade, the charge separations caused by the CME and the CMW have been carefully sought by the STAR [26–37], ALICE [38–41], and CMS [42–44] experiments at different collision energies and systems with multiple observables. Though early data suggest some hints matching

*shouqiye@fudan.edu.cn

†panos.christakoglou@nikhef.nl

‡mayugang@fudan.edu.cn

theoretical expectations, it is soon found that the background effects play a dominant role in experimental measurements. In both CME and CMW studies, for instance, the observables dramatically vary as v_2 changes [40,45], indicating significant contributions from the interplay between the way particles are being produced in pairs of oppositely charged partners, referred to as local charge conservation (LCC) and collective flow. Accounting for this background in the measurement reveals that the signal is consistent with zero within uncertainties. To understand the background and to disentangle the signal, various theoretical and phenomenological models containing different background and signal sources are developed to interpret the data, such as AVFD [46–48], AMPT [49–51]. These models succeed in describing some aspects of the measurements while, unfortunately, fail in others. A one-size-fits-all description reasonably coinciding with most experimental observables remains incomplete.

The CME and the CMW are usually treated as two independent analyses up to now, via methods in Eqs. (1) and (2), respectively. Even though the collectivity-convolved LCC is now clearly realized to be the background for both, no attempt has been made yet to unify the studies of the CME and the CMW, in particular, to estimate a comprehensive background in a realistic environment comparable to experimental data. In this Letter, we present simulation results using a modified blast wave (BW) model [52,53] at LHC energy. We will show that, when most global observables (p_T spectrum, v_2 , and, in particular, charge balance function) are tailored to describe experimental measurements (the data-driven way), the CME and CMW observables (e.g., $\Delta\gamma$, $\Delta\delta$, A_{ch} - v_2 slope) can be simultaneously and naturally reproduced. Based on that, the maximum allowable strength of the signal for both CME and CMW is further deduced through a phenomenological method, which sheds new light on the search for anomalous chiral effects.

Methodology. The blast wave model is extensively used in heavy-ion collisions [52,53], providing a convenient and straightforward way to describe the production of particles as well as their collective motions. It generates an expanding and locally thermalized fireball, which decays into fragments and subsequently emits hadrons. The thermal equilibrium of hadrons is based on the Boltzmann distribution with kinetic freeze-out temperature T_{kin} . The phase space distribution of the fragments is determined on the assumption that the radial expansion velocity is proportional to the distance from the center of the system. The initial shape of the fireball is controlled by a geometry parameter R_x/R_y describing the spacial asymmetry and the collectivity is determined by the radial flow parameter ρ_0 and the elliptic flow parameter ρ_2 in form of $\rho \cos(2\phi)$ with ϕ being the boost angle. For simplicity, higher order flow components are omitted since v_2 is the leading-order term and all particles are set to have pion mass.

It is worth noting that the BW does not include any evolution process, which is not the goal of this work either. Here, the BW simply serves as a generator, providing a decent description of basic features of the event, which could be replaced by other models with similar functions. This study is performed in Pb-Pb collisions at $\sqrt{s_{NN}} = 5.02$ TeV and the aforementioned parameters are listed in the top four rows

of Table I, with which the basic feature of p_T distribution and v_2 measured by ALICE experiment [54,55] can be well reproduced. For instance, the mean values of calculated integrated v_2 within $p_T < 2$ GeV/c and $|\eta| < 0.8$ at 5–10 %, 30–40 %, 50–60 % centrality intervals are 0.035, 0.081, 0.078, respectively, with negligible statistical uncertainties, matching experimental values [55] within 3% relative deviations.

Of particular importance for this work is the joint treatment of the multiplicity and the balancing charge. A realistic multiplicity value is usually taken into account for the study of particle production, however, is sometimes ignored for studies of correlations. For charge dependent correlations, we argue that a comparable multiplicity is significantly important because of two reasons: (I) In the CME study, the transverse momentum conservation (TMC) plays a non-negligible role. As pointed out in Refs. [56,57], inclusive γ and δ can be written into $\langle \cos \phi \rangle^2 - \langle \sin \phi \rangle^2 - v_2/N$ and $\langle \cos \phi \rangle^2 + \langle \sin \phi \rangle^2 - 1/N$, respectively, with $\langle \rangle$ being the event average. It is obvious that both $\langle \sin \phi \rangle$ and $\langle \cos \phi \rangle$ obey the law of large numbers (the central limit theorem as well), which manifests itself through the multiplicity. Events with high or low multiplicity (tight or loose TMC condition), therefore, naturally give rise to different γ and δ results. (II) In the CMW study, as shown in Eq. (2), the A_{ch} is a key observable determining the signal. By definition, the A_{ch} follows a negative binomial (NBD) distribution. The larger the multiplicity is, the narrower the A_{ch} distribution would be. Here, in each centrality, we sample the multiplicity event by event following the NBD with mean and variance from the ALICE results [54]. It will be shown later that the A_{ch} distribution can be precisely reproduced.

It is well known that, in heavy-ion collisions, for every produced particle in a specific phase space window, there should be a corresponding antiparticle with the opposite charge, which is commonly quantified by the balance function [58]. To introduce such a local charge dependent correlation, particles are emitted in pairs with conserved charge (one positively and one negatively charged) at some spatial points which are uniformly distributed within an ellipse, as illustrated in Fig. 1. The momenta of particles in a given pair are independently sampled and then boosted together so particles eventually follow a common collective velocity. For the rest of the spatial points, only one particle is generated with random charge. The percentage of points emitting pairs, f_{LCC} , is used to parametrize the strength of LCC. We tune the value of f_{LCC} in each centrality to match the experimental result of charge balance function, e.g., in 30–40 %, the $f_{LCC} = 0.54$ gives the width of the balance function of 0.64 ± 0.014 , which is consistent with the ALICE measurement [59–61] within 5% relative deviations. Note that the f_{LCC} decreases as collision goes from central to peripheral, indicating that the charge correlation gradually becomes weak, matching the ALICE measurement [61] (see Supplemental Material in [62] for more discussions). Since the evolution is not taken into account, we treat primordial particles following the LCC and resonances as a same kind of source. This is acceptable because, from the standpoint of final observables, both of them are clusters emitting a pair of correlated positive and negative particles. Moreover, nonflow effects were recently proposed

TABLE I. List of the modified BW parameters for Pb-Pb collisions at $\sqrt{s_{NN}} = 5.02$ TeV.

Centrality	0–5 %	5–10 %	10–20 %	20–30 %	30–40 %	40–50 %	50–60 %	60–70 %
T_{kin}	111.34	106.96	104.78	107.37	111.63	115.14	118.14	128.20
R_x/R_y	0.956	0.934	0.905	0.872	0.845	0.823	0.807	0.786
ρ_0	1.262	1.267	1.254	1.226	1.196	1.148	1.087	0.994
ρ_2	0.054	0.063	0.11	0.135	0.15	0.145	0.121	0.115
$N_{\text{ch}}(\eta < 0.8)$	2290	1858	1334	904	608	369	222	117
f_{LCC}	0.71	0.62	0.58	0.56	0.54	0.48	0.47	0.46

to play roles in the measurement, however, mainly in RHIC energy [63]. In TeV scale, it may be largely diluted by the high multiplicity so it is also ignored here.

CME and CMW observables. Figure 2 presents the CME observables $\Delta\gamma$ and $\Delta\delta$ as functions of centrality on the basis of the aforementioned model configuration. It is not surprising that the ALICE measured $\Delta\delta$ can be perfectly described by the model since, as mentioned in [41,64], $\Delta\delta$ is an equivalent form of the charge balance function. More importantly, the calculated $\Delta\gamma$ values are found to be quantitatively in line with ALICE data as well within 5% relative deviations in central and semicentral collisions. In the most peripheral collisions, the deviation increases to 10%, mainly owing to the fluctuation at low multiplicity. In Ref. [41], ALICE performed a similar comparison and found that when tuning the BW model to match the measured $\Delta\delta$, the model underestimates the measured $\Delta\gamma$ by around 40%. We would like to point out that such a discrepancy actually comes from the incomplete treatment of the LCC fraction and the multiplicity. With such

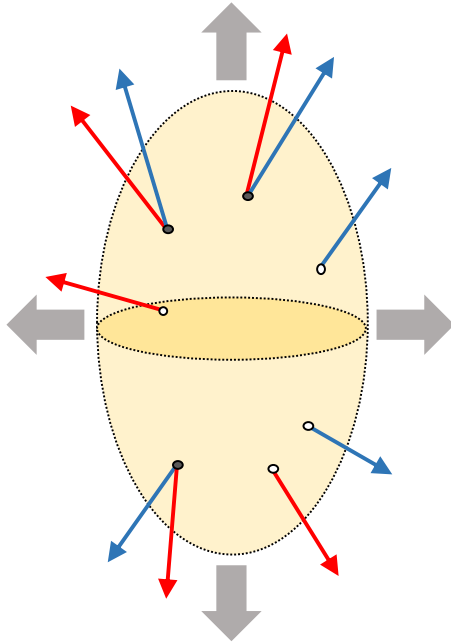


FIG. 1. A schematic view of a BW event with improved treatment of the LCC. Grey arrows indicate the collective expansion. Positive and negative charges are marked in red and blue respectively. Open and full circles denote the single particle production and the pair production, respectively.

an issue being properly addressed, a quantitative description of both $\Delta\delta$ and $\Delta\gamma$ can be achieved.

In addition to the CME study, the BW+LCC model has also been used for the study of CMW. As demonstrated in our early work [65], when selecting events with a specific A_{ch} , in practice, one preferentially applies nonuniform kinematic cuts on charged particles and such a LCC background is too ubiquitous to be eliminated. The underlying mechanism has also been clearly discussed in Refs. [66–68]. Nevertheless, an accurate estimation remains unexplored. Figure 3 shows the calculated normalized slope of $A_{\text{ch}}-\Delta v_2$ in this model. It can be seen that the slope values match the ALICE measurement within 12% relative deviation. The centrality dependence can be naturally described as well: the slight decrease of the slope is due to the smaller number of balancing pairs when collisions becomes more peripheral. As a detailed example, the linear dependence between v_2^\pm and A_{ch} and the A_{ch} distribution in 30–40 % centrality are attached in the embedded panels (a) and (b), respectively. Note that the A_{ch} distribution is in good accord with the ALICE result [45], supporting our explanation in the previous section.

The set of parameters summarized in Table I may not be the only viable configuration, however, given the fact that the small experimental uncertainty of $\Delta\gamma$ ($\approx 10^{-4}$) imposes a strong constraint on the model, there is little room for those parameters to change.

Taken together, the consistency between the modified BW model and the ALICE data suggests that the current experimental measurements of anomalous chiral effects can be reasonably explained by a simple and realistic LCC

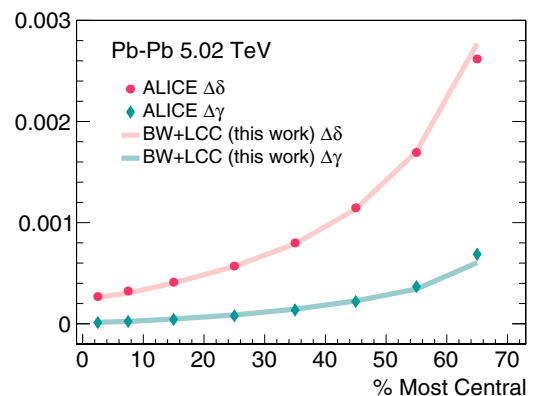


FIG. 2. The CME observables $\Delta\gamma$ and $\Delta\delta$ as functions of centrality. The ALICE results are from [41].

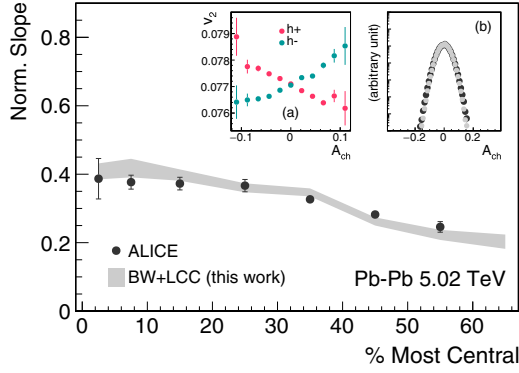


FIG. 3. The CMW observable, normalized slope of $A_{ch} - \Delta v_2$, as a function of centrality. The ALICE results are from [45]. Insets: (a) the linear dependence between v_2^{\pm} and A_{ch} , (b) A_{ch} distribution, in 30–40 % centrality.

background. Nevertheless, it does not yet rule out signals of the CME and the CMW. Even though the signals are widely believed to be small [69], from the perspective of observables, there is a possibility that, in principle, both CME and CMW can exist concurrently together with a slightly weaker LCC background. On the basis of the model with a comprehensive understanding of the background, we take one step further to determine the maximum allowable strength of signals by introducing charge separations in a phenomenological approach.

Constraint on the Signal. In previous AMPT studies [50,51], the y component of the momentum (position) coordinate for some “above-plane” (in-plane) particles carrying a given charge are randomly interchanged with those “below-plane” (out-of-plane) ones carrying the opposite charge to mimic the CME (CMW) signal. Such a straightforward operation has proven to be fairly effective. In this work, it should be emphasized that, instead of switching particles’ positions or momenta, we simply interchange their charges, which is indeed equivalent to the former when the evolution is not taken into account. Specifically, only charges of those single-produced particles, denoted by white dots in Fig. 1, are swapped following the above mentioned method, while the pair-produced ones remain unchanged so the LCC background can be separately under control. Figures 4(b), 4(c), and 4(d) show the net electric charge distributions in the transverse plane after incorporating signals of the CME, the CMW, and a superposition of both, respectively. It is easy to prove that two kinds of signals are independent, namely, the CME signal has no effect on the CMW observable and vice versa, so the superposition can be decomposed without mutual interaction. Note that the signals in Fig. 4 are intentionally enhanced for better visualization and only one of two dipole and quadrupole configurations is presented as an example. The strengths of both signals, S_{CME} and S_{CMW} , are quantified by the number of pairs being interchanged. Our goal is to quantitatively find out the maximum strength of signal that can be tolerated within experimental precision.

The influences of four key parameters (multiplicity, f_{LCC} , S_{CME} , and S_{CMW}) on three observables ($\Delta\delta$, $\Delta\gamma$, and the

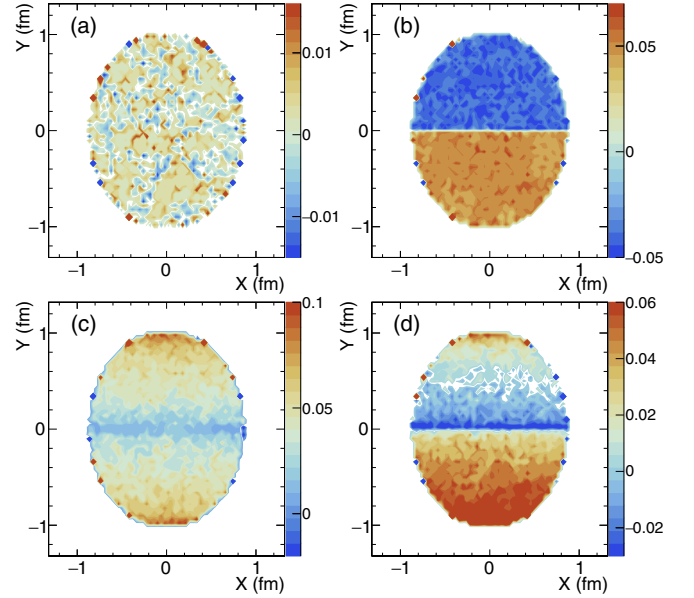


FIG. 4. The net electric charge distributions in the transverse plane when the signal is (a) not imported, (b) imported to mimic the CME-induced dipole moment, (c) imported to mimic the CMW-induced quadrupole moment, (d) imported to mimic a superposed effect of both CME and CMW. Signals are intentionally enhanced here for better visualization.

slope) are summarized in Table II. First, to accommodate both signals, which increase the $\Delta\gamma$ and the slope, the f_{LCC} must be reduced. However, this will lead to the further decrease of the $\Delta\delta$. Consequently, as a compensation, the multiplicity needs to be reduced as well, which is the only viable solution for making the signal and the background coexist. Note that the multiplicity is a robust observable rather than a freely adjustable parameter but the measurement allows up to 10% uncertainty around the mean values [54]. Therefore, we reduce the multiplicity by a few percent ($< 10\%$) in each centrality, ensuring that the A_{ch} distribution remains comparable to the data. With the fixed multiplicity, the f_{LCC} is then tweaked as small as it can go to match the limits of the measured charge balance function and the $\Delta\delta$. Compared to the values in Table I, f_{LCC} are diminished by $\approx 15\%$, $\approx 10\%$, and $\approx 1\%$ in the most central, the semicentral, and the peripheral collisions, respectively.

In the absence of the LCC background, i.e., when all particles are single-produced, it is discovered that the natural charge fluctuation can produce a $\Delta\delta$ and a $\Delta\gamma$ on the order of $\approx 10^{-7}$ – 10^{-6} , serving as a baseline. Swapping the charge once to create one pair of dipole moment is able to generate

TABLE II. The impact of four key parameters on the CME and the CMW observables.

	$\Delta\delta$	$\Delta\gamma$	Slope
Mult. \searrow	\nearrow	\nearrow	–
f_{LCC} \searrow	\searrow	\searrow	\searrow
S_{CME} \nearrow	\searrow	\nearrow	–
S_{CMW} \nearrow	–	–	\nearrow

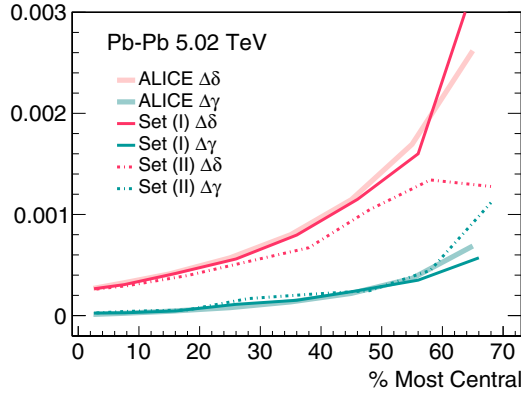


FIG. 5. The CME observables $\Delta\gamma$ and $\Delta\delta$ as functions of centrality when the signal is imported. Set (I) is still comparable with the ALICE data while set (II) is not, indicating the maximum allowable strength.

a $\Delta\delta \approx -10^{-5}$ and a $\Delta\gamma \approx 10^{-5}$. Since the variation of $\Delta\delta$ and $\Delta\gamma$ is simply proportional to the interchange time, S_{CME} , following the rule of S_{CME}^2 , switching three times will almost increase the observables by one order of magnitude. Similarly, creating one quadrupole gives rise to the $\Delta v_2 \approx 10^{-3}$ when $A_{\text{ch}} \approx \pm 0.1$, and the further variation follows the rule of $2S_{\text{CMW}}$. These simple rules serve as reference when adding the signal.

Two sets of CME signal, (I) and (II), are implemented. In set (I), the S_{CME} is linearly related to the multiplicity, so the values vary event by event from 1 to 3 for central and semicentral collisions and from 0 to 1 for peripheral collisions. In set (II), the S_{CME} is fixed to 3 (1) for central and semicentral (peripheral) collisions. Figure 5 shows the comparison between two sets and the ALICE data. It is obvious to see that the finely tuned set (I) is still roughly consistent with the data. However, the fixed set (II), providing signals over much, fails, in particular for peripheral collisions, which indicates that the signal does not likely to appear there. The deviation from data continues to increase as the S_{CME} grows. In 30–40 % centrality, the mean S_{CME} value is ≈ 1 and the net CME-induced $\Delta\gamma$ when $S_{\text{CME}} = 1$ is 2×10^{-5} . Compared to the total $\Delta\gamma$ of 1.5×10^{-4} , therefore, the allowable maximum fraction of CME signal should be no more than $\approx 13\%$. Likewise, the average allowable S_{CMW} in 30–40 % centrality is ≈ 0.5 , meaning that one signal is permitted in every two events, and the calculated maximum fraction of CMW in the slope is found to be $\approx 2\%$. A larger signal, e.g., $S_{\text{CMW}} = 1$, would result in the increase of the slope by a factor of 3. Note that such estimations do not take any measuring factor into account. Considering various experimental uncertainties (detector-wise and methodology-wise), the final measured signals, even existing, would be further reduced. In a word, any experimental results larger than these upper limits

might be unreasonable and there are very few opportunities to capture such tiny signals in LHC energy, matching the current ALICE and CMS conclusions.

Conclusion. In heavy-ion collisions, when studying the charge dependent correlations to search for anomalous chiral effects, the LCC effect is recognized as one of the most important backgrounds. Meanwhile, the CME and the CMW, despite sharing a similar background mechanism, have always been handled as two separate analyses. In this Letter, we present a simulation using a modified BW model, which naturally describes most experimental results, including the CME and the CMW observables, at the same time. Such a universal description, unifies the CME and the CMW studies and quantitatively reveals the connections between the observable, the signal and the LCC background. Following the *principle of parsimony*, we argue that, in LHC energy, the measured results of both the CME and the CMW can be interpreted to a great extent by the LCC entwined with the collective flow. We then propose a phenomenological approach of incorporating the CME and the CMW signals to quantify the maximum allowable strength of the signal. Our calculation shows that the CME and CMW fractions in the observables, even in the most ideal condition, should be no more than 13% and 2%, respectively. Such a global constraint provides a fresh perspective to understand the experimental data.

The BW model is quite straightforward and the realistic environment is obviously more complicated. However, the calculation in this work is tightly based on experimental results and the success of this model, particularly in unifying the CME and the CMW observables, may enlighten other more fundamental studies. We strongly suggest that this method, after being properly modified, should be extended to RHIC energy, where signals are expected to be stronger due to possibly longer life time of the magnetic field, to further nail down the interpretation. It is also desirable to introduce identified particles to investigate more subtle correlations.

Acknowledgments. We are grateful to our collaborators in the ALICE and the STAR experiments for enlightening discussions and suggestions. We appreciate J. Liao for helpful comments from theoretical standpoint. We also thank W.-B. He and C. Zhong for their effort on maintaining computing resources. This work is supported by the National Key Research and Development Program of China (Grants No. 2018YFE0104600, No. 2016YFE0100900), the National Natural Science Foundation of China (Grants No. 11890710, No. 11890714, No. 12061141008, No. 11975078, No. 11421505), the Strategic Priority Research Program of Chinese Academy of Sciences (Grant No. XDB34030000), and the Guangdong Major Project of the Guangdong Major Project of Basic and Applied Basic Research (Grant No. 2020B0301030008). Q.-Y.S. is also sponsored by the Shanghai Rising-Star Program (Grant No. 20QA1401500).

[1] T. Lee, A theory of spontaneous T violation, *Phys. Rev. D* **8**, 1226 (1973).

[2] T. Lee and G. Wick, Vacuum stability and vacuum excitation in a spin 0 field theory, *Phys. Rev. D* **9**, 2291 (1974).

- [3] P. Morley and I. Schmidt, Strong P, CP, T violations in heavy ion collisions, *Z. Phys. C* **26**, 627 (1985).
- [4] D. Kharzeev, R. D. Pisarski, and M. H. G. Tytgat, Possibility of Spontaneous Parity Violation in Hot QCD, *Phys. Rev. Lett.* **81**, 512 (1998).
- [5] D. Kharzeev and R. D. Pisarski, Pionic measures of parity and CP violation in high-energy nuclear collisions, *Phys. Rev. D* **61**, 111901(R) (2000).
- [6] D. E. Kharzeev, Topology, magnetic field, and strongly interacting matter, *Annu. Rev. Nucl. Part. Sci.* **65**, 193 (2015).
- [7] D. Kharzeev and A. Zhitnitsky, Charge separation induced by P-odd bubbles in QCD matter, *Nucl. Phys. A* **797**, 67 (2007).
- [8] D. E. Kharzeev, L. D. McLerran, and H. J. Warringa, The Effects of topological charge change in heavy ion collisions: Event by event P and CP violation, *Nucl. Phys. A* **803**, 227 (2008).
- [9] K. Fukushima, D. E. Kharzeev, and H. J. Warringa, The chiral magnetic effect, *Phys. Rev. D* **78**, 074033 (2008).
- [10] V. Skokov, A. Illarionov, and V. Toneev, Estimate of the magnetic field strength in heavy-ion collisions, *Int. J. Mod. Phys. A* **24**, 5925 (2009).
- [11] A. Bzdak and V. Skokov, Event-by-event fluctuations of magnetic and electric fields in heavy ion collisions, *Phys. Lett. B* **710**, 171 (2012).
- [12] W.-T. Deng and X.-G. Huang, Event-by-event generation of electromagnetic fields in heavy-ion collisions, *Phys. Rev. C* **85**, 044907 (2012).
- [13] S. A. Voloshin, Parity violation in hot QCD: How to detect it, *Phys. Rev. C* **70**, 057901 (2004).
- [14] D. Kharzeev, Parity violation in hot QCD: Why it can happen, and how to look for it, *Phys. Lett. B* **633**, 260 (2006).
- [15] F.-Q. Wang and J. Zhao, Search for the chiral magnetic effect in heavy ion collisions, *Nucl. Sci. Tech.* **29**, 179 (2018).
- [16] Y. Burnier, D. E. Kharzeev, J. Liao, and H.-U. Yee, Chiral Magnetic Wave at Finite Baryon Density and the Electric Quadrupole Moment of the Quark-Gluon Plasma, *Phys. Rev. Lett.* **107**, 052303 (2011).
- [17] Y. Burnier, D. E. Kharzeev, J. Liao, and H. U. Yee, From the chiral magnetic wave to the charge dependence of elliptic flow, [arXiv:1208.2537](https://arxiv.org/abs/1208.2537).
- [18] S. F. Taghavi and U. A. Wiedemann, Chiral magnetic wave in an expanding QCD fluid, *Phys. Rev. C* **91**, 024902 (2015).
- [19] H.-U. Yee and Y. Yin, Realistic implementation of chiral magnetic wave in heavy ion collisions, *Phys. Rev. C* **89**, 044909 (2014).
- [20] D. E. Kharzeev, J. Liao, S. A. Voloshin, and G. Wang, Chiral magnetic and vortical effects in high-energy nuclear collisions—A status report, *Prog. Part. Nucl. Phys.* **88**, 1 (2016).
- [21] K. Hattori and X.-G. Huang, Novel quantum phenomena induced by strong magnetic fields in heavy-ion collisions, *Nucl. Sci. Tech.* **28**, 26 (2017).
- [22] J. Zhao and F. Wang, Experimental searches for the chiral magnetic effect in heavy-ion collisions, *Prog. Part. Nucl. Phys.* **107**, 200 (2019).
- [23] Y.-C. Liu and X.-G. Huang, Anomalous chiral transports and spin polarization in heavy-ion collisions, *Nucl. Sci. Tech.* **31**, 56 (2020).
- [24] J.-H. Gao, G.-L. Ma, S. Pu, and Q. Wang, Recent developments in chiral and spin polarization effects in heavy-ion collisions, *Nucl. Sci. Tech.* **31**, 90 (2020).
- [25] J. Liao, V. Koch, and A. Bzdak, Charge separation effect in relativistic heavy ion collisions, *Phys. Rev. C* **82**, 054902 (2010).
- [26] B. I. Abelev *et al.* (STAR Collaboration), Azimuthal Charged-Particle Correlations and Possible Local Strong Parity Violation, *Phys. Rev. Lett.* **103**, 251601 (2009).
- [27] B. I. Abelev *et al.* (STAR Collaboration), Observation of charge-dependent azimuthal correlations and possible local strong parity violation in heavy ion collisions, *Phys. Rev. C* **81**, 054908 (2010).
- [28] L. Adamczyk *et al.* (STAR Collaboration), Fluctuations of charge separation perpendicular to the event plane and local parity violation in $\sqrt{s_{NN}} = 200$ GeV Au+Au collisions at the BNL Relativistic Heavy Ion Collider, *Phys. Rev. C* **88**, 064911 (2013).
- [29] L. Adamczyk *et al.* (STAR Collaboration), Beam-Energy Dependence of Charge Separation Along the Magnetic Field in Au+Au Collisions at RHIC, *Phys. Rev. Lett.* **113**, 052302 (2014).
- [30] J. Adam *et al.* (STAR Collaboration), Charge-dependent pair correlations relative to a third particle in $p+$ Au and $d+$ Au collisions at RHIC, *Phys. Lett. B* **798**, 134975 (2019).
- [31] J. Adam *et al.* (STAR Collaboration), Methods for a blind analysis of isobar data collected by the STAR collaboration, *Nucl. Sci. Tech.* **32**, 48 (2021).
- [32] M. Abdallah *et al.* (STAR Collaboration), Search for the chiral magnetic effect with isobar collisions at $\sqrt{s_{NN}}=200$ GeV by the STAR Collaboration at the BNL Relativistic Heavy Ion Collider, *Phys. Rev. C* **105**, 014901 (2022).
- [33] M. S. Abdallah *et al.* (STAR Collaboration), Search for the Chiral Magnetic Effect via Charge-Dependent Azimuthal Correlations Relative to Spectator and Participant Planes in Au+Au Collisions at $\sqrt{s_{NN}} = 200$ GeV, *Phys. Rev. Lett.* **128**, 092301 (2022).
- [34] S. Choudhury *et al.*, Investigation of experimental observables in search of the chiral magnetic effect in heavy-ion collisions in the STAR experiment*, *Chin. Phys. C* **46**, 014101 (2022).
- [35] L. Adamczyk *et al.* (STAR Collaboration), Observation of Charge Asymmetry Dependence of Pion Elliptic Flow and the Possible Chiral Magnetic Wave in Heavy-Ion Collisions, *Phys. Rev. Lett.* **114**, 252302 (2015).
- [36] STAR Collaboration, Search for the chiral magnetic wave using anisotropic flow of identified particles at RHIC, [arXiv:2210.14027](https://arxiv.org/abs/2210.14027).
- [37] H.-j. Xu, J. Zhao, Y. Feng, and F. Wang, Importance of non-flow background on the chiral magnetic wave search, *Nucl. Phys. A* **1005**, 121770 (2021).
- [38] B. Abelev *et al.* (ALICE Collaboration), Charge Separation Relative to the Reaction Plane in Pb-Pb Collisions at $\sqrt{s_{NN}} = 2.76$ TeV, *Phys. Rev. Lett.* **110**, 012301 (2013).
- [39] J. Adam *et al.* (ALICE Collaboration), Charge-dependent flow and the search for the chiral magnetic wave in Pb-Pb collisions at $\sqrt{s_{NN}} = 2.76$ TeV, *Phys. Rev. C* **93**, 044903 (2016).
- [40] S. Acharya *et al.* (ALICE Collaboration), Constraining the magnitude of the chiral magnetic effect with event shape engineering in Pb-Pb collisions at $\sqrt{s_{NN}} = 2.76$ TeV, *Phys. Lett. B* **777**, 151 (2018).
- [41] S. Acharya *et al.* (ALICE Collaboration), Constraining the chiral magnetic effect with charge-dependent azimuthal correlations in Pb-Pb collisions at $\sqrt{s_{NN}} = 2.76$ and 5.02 TeV, *J. High Energy Phys.* **09** (2020) 160.

- [42] A. M. Sirunyan *et al.*, (CMS Collaboration), Probing the chiral magnetic wave in pPb and PbPb collisions at $\sqrt{s_{NN}} = 5.02$ TeV using charge-dependent azimuthal anisotropies, *Phys. Rev. C* **100**, 064908 (2019).
- [43] A. M. Sirunyan *et al.*, (CMS Collaboration), Constraints on the chiral magnetic effect using charge-dependent azimuthal correlations in pPb and PbPb collisions at the CERN Large Hadron Collider, *Phys. Rev. C* **97**, 044912 (2018).
- [44] V. Khachatryan *et al.*, (CMS Collaboration), Observation of Charge-Dependent Azimuthal Correlations in p -Pb Collisions and its Implication for the Search for the Chiral Magnetic Effect, *Phys. Rev. Lett.* **118**, 122301 (2017).
- [45] W. Wu, <https://indico.cern.ch/event/1037821/contributions/4841755/>, talk given at SQM 2022 for the ALICE Collaboration, proceedings in preparation.
- [46] S. Shi, H. Zhang, D. Hou, and J. Liao, Chiral magnetic effect in isobaric collisions from anomalous-viscous fluid dynamics (AVFD), *Nucl. Phys. A* **982**, 539 (2019).
- [47] S. Shi, H. Zhang, D. Hou, and J. Liao, Signatures of Chiral Magnetic Effect in the Collisions of Isobars, *Phys. Rev. Lett.* **125**, 242301 (2020).
- [48] P. Christakoglou, S. Qiu, and J. Staa, Systematic study of the chiral magnetic effect with the AVFD model at LHC energies, *Eur. Phys. J. C* **81**, 717 (2021).
- [49] Z.-W. Lin, C. M. Ko, B.-A. Li, B. Zhang, and S. Pal, A Multi-phase transport model for relativistic heavy ion collisions, *Phys. Rev. C* **72**, 064901 (2005).
- [50] G.-L. Ma and B. Zhang, Effects of final state interactions on charge separation in relativistic heavy ion collisions, *Phys. Lett. B* **700**, 39 (2011).
- [51] G.-L. Ma, Final state effects on charge asymmetry of pion elliptic flow in high-energy heavy-ion collisions, *Phys. Lett. B* **735**, 383 (2014).
- [52] F. Retiere and M. A. Lisa, Observable implications of geometrical and dynamical aspects of freeze out in heavy ion collisions, *Phys. Rev. C* **70**, 044907 (2004).
- [53] B. Tomášik, DRAGON: Monte Carlo generator of particle production from a fragmented fireball in ultrarelativistic nuclear collisions, *Comput. Phys. Commun.* **180**, 1642 (2009).
- [54] S. Acharya *et al.* (ALICE Collaboration), Production of charged pions, kaons, and (anti-)protons in Pb-Pb and inelastic pp collisions at $\sqrt{s_{NN}} = 5.02$ TeV, *Phys. Rev. C* **101**, 044907 (2020).
- [55] S. Acharya *et al.* (ALICE Collaboration), Energy dependence and fluctuations of anisotropic flow in Pb-Pb collisions at $\sqrt{s_{NN}} = 5.02$ and 2.76 TeV, *J. High Energy Phys.* **07** (2018) 103.
- [56] S. Pratt, S. Schlichting, and S. Gavin, Effects of momentum conservation and flow on angular correlations at RHIC, *Phys. Rev. C* **84**, 024909 (2011).
- [57] A. Bzdak, V. Koch, and J. Liao, Azimuthal correlations from transverse momentum conservation and possible local parity violation, *Phys. Rev. C* **83**, 014905 (2011).
- [58] S. A. Bass, P. Danielewicz, and S. Pratt, Clocking Hadronization in Relativistic Heavy-Ion Collisions with Balance Functions, *Phys. Rev. Lett.* **85**, 2689 (2000).
- [59] B. Abelev *et al.* (ALICE Collaboration), Charge correlations using the balance function in Pb-Pb collisions at $\sqrt{s_{NN}} = 2.76$ TeV, *Phys. Lett. B* **723**, 267 (2013).
- [60] J. Adam *et al.* (ALICE Collaboration), Multiplicity and transverse momentum evolution of charge-dependent correlations in pp, p-Pb, and Pb-Pb collisions at the LHC, *Eur. Phys. J. C* **76**, 86 (2016).
- [61] S. Acharya *et al.* (ALICE Collaboration), General balance functions of identified charged hadron pairs of (π , K, p) in Pb-Pb collisions at sNN= 2.76 TeV, *Phys. Lett. B* **833**, 137338 (2022).
- [62] See Supplemental Material at <http://link.aps.org/supplemental/10.1103/PhysRevC.107.L031902> for more discussions regarding the connection between the parameter f_{LCC} in this work and the ALICE measurement of the charge balance function. more discussions.
- [63] Y. Feng, J. Zhao, H. Li, H.-j. Xu, and F. Wang, Two- and three-particle nonflow contributions to the chiral magnetic effect measurement by spectator and participant planes in relativistic heavy ion collisions, *Phys. Rev. C* **105**, 024913 (2022).
- [64] Y. Hori, T. Gunji, H. Hamagaki, and S. Schlichting, Collective flow effects on charge balance correlations and local parity-violation observables in $\sqrt{s_{NN}} = 2.76$ TeV Pb+Pb collisions at the LHC, [arXiv:1208.0603](https://arxiv.org/abs/1208.0603).
- [65] C.-Z. Wang, W.-Y. Wu, Q.-Y. Shou, G.-L. Ma, Y.-G. Ma, and S. Zhang, Interpreting the charge-dependent flow and constraining the chiral magnetic wave with event shape engineering, *Phys. Lett. B* **820**, 136580 (2021).
- [66] A. Bzdak and P. Bozek, Contributions to the event-by-event charge asymmetry dependence for the elliptic flow of pi^+ and pi^- in heavy-ion collisions, *Phys. Lett. B* **726**, 239 (2013).
- [67] S. A. Voloshin and R. Belmont, Measuring and interpreting charge dependent anisotropic flow, *Nucl. Phys. A* **931**, 992 (2014).
- [68] W.-Y. Wu, C.-Z. Wang, Q.-Y. Shou, Y.-G. Ma, and L. Zheng, Charge-dependent transverse momentum and its impact on the search for the chiral magnetic wave, *Phys. Rev. C* **103**, 034906 (2021).
- [69] B. Müller and A. Schafer, Charge fluctuations from the chiral magnetic effect in nuclear collisions, *Phys. Rev. C* **82**, 057902 (2010).